THE JOURNAL OF PHYSICAL CHEMISTRY Letters

Letter

Cite This: J. Phys. Chem. Lett. 2019, 10, 1729−1736

pubs.acs.org/JPCL

How β-Phase Content Moderates Chain Conjugation and Energy Transfer in Polyfluorene Films

Hannah J. Eggimann, Florian Le Roux, and Laura M. Herz*

Department of Physics, University of Oxford, Clarendon Laboratory, Parks Road, Oxford OX1 3PU, United Kingdom

Supporting Information

ABSTRACT: Poly(9,9-dioctylfluorene) (PFO) is a blue-light-emitting polymer exhibiting two distinct phases, namely, the disordered "glassy" phase and a more ordered β-phase. We investigate how a systematic increase in the fraction of β-phase present in PFO films controls chain conformation, photoluminescence quantum efficiency (PLQE), and the resonant energy transfer from the glassy to the β-phase. All films are prepared by the same technique, using paraffin oil as an additive to the spin-coating solution, allowing systematic tuning of the β-phase fraction. The PFO films exhibit high PLQE with values increasing to 0.72 for increasing fractions of β-phase present, with the β-phase chain conformation becoming more planar and including more repeat units. Differences in Förster radii calculated from the overlap of steady-state absorptance and emission spectra and from time-resolved ultrafast photoluminescence transients indicate that exciton diffusion within the glassy phase plays an important role in the energy transfer process.

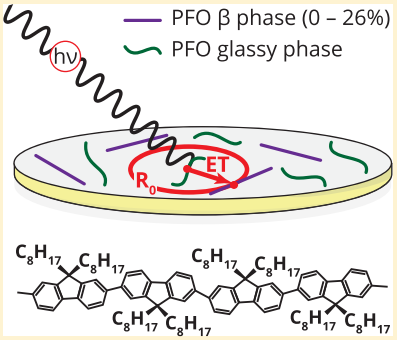

Semiconducting conjugated polymers are a rising class of materials offering tunable electrical and optical properties combined with the attractive prospect of low-cost and large-scale device fabrication.[1−5] One widely explored polymer in this context is poly(9,9-dioctylfluorene) (PFO), a member of the family of fluorene-based polymers that have found widespread use in a range of applications including organic light emitting diodes (OLEDs),[6−8] transistors,[9] and lasers.[10,11] PFO features desirable photo- and electroluminescence[7,12,13] as well as high optical gain and respectable charge-carrier mobilities.[14] It is known to adopt two distinct phases, namely, the disordered "glassy" phase and the more crystalline β-phase,[15−19] which differ by the angles adopted between neighboring fluorene units. For the glassy phase, these angles vary randomly within a large spread of possible values, while they take a set value of 180° in the β-phase, corresponding to a coplanar, extended, and more rigid chain conformation.[16,19] Inclusion of polymer chains that have adopted β-phase conformation appears to have a beneficial impact on optoelectronic properties of PFO films, such as improved spectral stability for emission[20] and efficient photoluminescence (PL).[8,13] While the absorption spectrum of PFO films typically reflects the sum over the distinct spectral contributions from glassy and β-phase conformations present, the emission spectrum is typically dominated by contributions from the β-phase, even for relatively minor inclusions. This observation led Ariu et al.[18,21] to the conclusion that, following excitation, energy is transferred efficiently from glassy-phase chain segments to β-phase chain segments. Such energy transfer was indeed found to occur on a sub-picosecond time scale for a PFO film with ∼25% β-phase content,[22] and it has since been a subject of further study.[23−25] However, a conclusive investigation of how such energy transfer depends on β-phase content for a reliably and widely tuned range of β-phase fractions is still outstanding.

High photoluminescence quantum efficiency (PLQE) is an essential requirement for the efficient use of conjugated polymers as light emission materials in display, lighting, and laser applications. A better understanding of the fundamental material properties determining PLQE is therefore of great importance. PFO provides a versatile platform for such studies, given the variation in polymer chain conformations that can be induced and explored. The introduction of some β-phase extended chain segments in PFO films has been found to improve emission performance.[7,8,12,13] Moreover, it has recently been observed that the PLQE of PFO films strongly depends on the fraction of β-phase chain segments contained,[8,13] with a record high PLQE measured for modest fractions (∼5−15%) of β-phase.[8,13,26] However, such studies have so far suffered from the use of different preparation methods employed along a series of films within a given range of β-phase fractions, which may have resulted in an undesirable influence of altered microstructure and defect content on PLQE. The use of one single preparation technique throughout the series, as in the study presented here, is therefore crucial in order for the effect of β-phase content on optoelectronic properties to be clearly isolated and investigated. The key reasons why the PLQE of PFO films depends on the fraction of β-phase chain segments[13] are therefore still a matter of some debate, with possible factors including alterations in film microstructure[27,28] and chain conformation,

Received: February 20, 2019
Accepted: March 22, 2019
Published: March 22, 2019

changes in the energy transfer mechanisms,[23,24,26] and their potential interplay.[29]

In this Letter, we explore how the fraction of β-phase chains present in PFO thin films affects the nature of the electronic states, the chain conformation, PLQE, and the Förster resonant energy transfer (FRET) from glassy to β-phase chain segments. To ensure consistency of results, we prepared PFO films with varying content of β-phase through one single preparation method. First, we probe changes in the electronic states and thereby the film microstructure by examining emission and absorptance spectra of films with varying β-phase fraction. An analysis of the PL spectra suggests that the length of the β-phase chain segments and/or their planarity increases as the β-phase fraction grows, enhancing the value of the PLQE. Second, we study the influence of the β-phase fraction on resonant energy transfer between glassy and β-phase chain segments. To this end, we determine Förster radii from spectral overlap calculations based on steady-state spectroscopic measurements, as well as from time-resolved ultrafast PL up-conversion spectroscopy. We show that resonant energy transfer does not become more efficient but is an overall faster process with increasing β-phase content. By comparing the values obtained from the two different methods, we find that the Förster radius is enhanced by exciton diffusion within the glassy phase occurring prior to energy transfer.

We prepared a series of PFO thin films with varying β-phase fractions by employing a novel technique recently proposed by Zhang et al.,[8] which uses paraffin oil as an additive to the solutions of polymer in toluene from which thin films are produced via spin-casting. Small amounts of paraffin (ranging between 0 and 0.4 vol % in toluene) were found to allow tuning of the fraction of β-phase content in the film between 0% and 25.6% (see Supporting Information Section 1 for full fabrication details). Importantly, this method enables the fabrication of a series of PFO films with widely varying β-phase content through one single technique. Such an approach is decisive for the comparability of measurements from films with a range of β-phase content, which has been identified as a concern in previous studies.[13] We determine the fraction of β-phase chain segments within the films from absorptance spectra (Figure S1) by deconvolution of the total absorptance spectra into contributions from the glassy and β-phase chain segments, from which the β-phase emission spectrum was obtained by subtraction of the normalized contribution from the glassy phase (Figure S3).[17,30] A detailed description of the method used to determine the fraction of β-phase chain segments in the films is given in Section 2 in Supporting Information.

We begin by exploring potential changes in chain conformation with increasing β-phase fraction in PFO films, by carefully examining their absorptance and emission spectra. In Figure 1a we show the normalized steady-state PL spectra for our PFO film series collected following illumination with 380 nm wavelength light, which predominantly excites the glassy phase. On the one hand, evidently the emission only resembles the spectrum expected for the glassy phase of PFO, when no substantial ($\leq$0.5%) β-phase is detectable in the corresponding absorptance spectra. For all films containing more than 0.5% β-phase, on the other hand, the PL spectra are dominated by the red-shifted emission from the β-phase, in accordance with previous observations,[13,21] and suggesting almost complete channeling of excitations from the glassy to the β-phase. The observed peak positions are consistent with

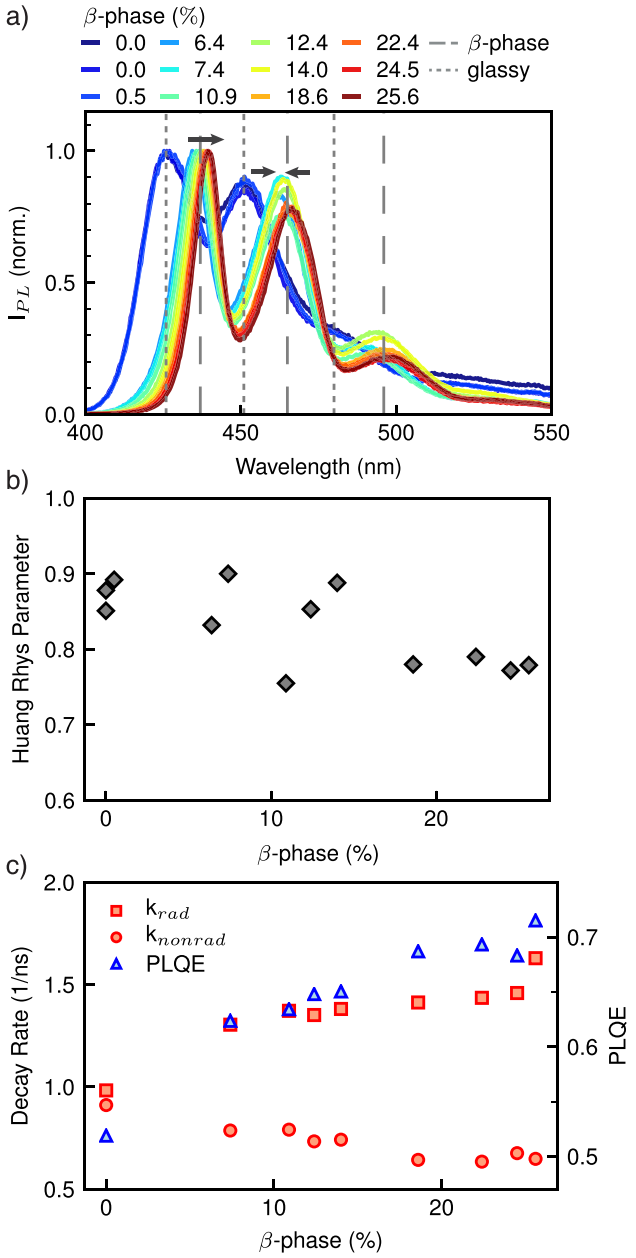

Figure 1. (a) Normalized time-integrated PL spectra for PFO films containing different fractions of β-phase chains ranging between 0% and 25.6%. The approximate positions of the vibronic emission peaks of the glassy and the β-phase are indicated by the dotted and dashed lines, respectively. All films were excited with light of wavelength 380 nm and intensity 200 μW. The arrows indicate the observed red shift and the peak narrowing as the β-phase fraction increases. (b) Huang–Rhys parameter, obtained from the ratio of the 0–0 and 0–1 PL peak heights. (c) PLQE (blue triangles, right axis), radiative (red squares, left axis) and nonradiative (red circles, left axis) PL decay rates. The rates were deduced from the PL lifetimes measured by TCSPC and the PLQE values, as described in Section S5.1 in the Supporting Information.

previous reports,[8,13,21] with the β-phase emission peak around 437 nm assigned to the $S_1 \rightarrow S_0$ 0–0 vibronic transition.[13,15,21]

Interestingly, closer examination of the PL spectra dominated by β-phase emission reveals that all vibronic peaks shift to the red with increasing fraction of β-phase chain segments in the film. The peak position of the 0–0 peak

DOI: 10.1021/acs.jpclett.9b00483
J. Phys. Chem. Lett. 2019, 10, 1729–1736

shifts by 5 nm from 435 to 440 nm, as the β-phase fraction increases from 6.4% to 25.6%. Even though shifts in PL peak position with β-phase content have been observed previously,[8,13,27] they have not yet been examined in detail[8,27] and considered to be an artifact caused by self-absorptance and/or changes in microstructural heterogeneity.[13] We may rule out self-absorption as the cause of the red shift here, because these shifts are also present for the 0−1 vibronic peak (located at wavelengths at which the films do not absorb), and they can as well be observed in the corresponding absorptance spectra (vide infra). Instead, we attribute the peak shift to a change in the excited electronic states with increasing β-phase content. Concomitantly, the vibronic emission peaks are found to become spectrally narrower with increasing β-phase content in the film (Figure S5 in Supporting Information). We suggest that both the shift of the emission peaks to lower energies and the decrease in spectral broadening arise from an increase in conjugation length and a more delocalized excited state.[31,32] Planarization[33] and an increase in oligomer length[34] in π-conjugated poly- and oligomers has been shown to result in red-shifted emission, which is a consequence of a highly delocalized excited state that is also less susceptible to energetic disorder arising from variations in conjugation length. Hence, our observations suggest that the β-phase chain segments become more planar and/or include more repeat units with increasing β-phase fraction in the film.

This conclusion is further supported by the associated trend in the Huang−Rhys parameter *S*, deduced from the intensity ratio of the 0−0 and 0−1 PL peaks and depicted in Figure 1b as a function of β-phase fraction. We observe a decrease in *S* with increasing β-phase content, which signifies a decrease in displacement from the ground-state equilibrium to the lowest excited-state geometry, with respect to the configuration coordinate associated with the C−C bond separation. Upon photoexcitation, the C−C bond alternation changes along the polymer backbone, as π-electrons are redistributed in a way that planarizes the backbone in the excited state. As a result, more planar geometries may yield smaller changes in conjugation coordinate upon excitation (decreased *S*). Studies of phenylenevinylene oligomers[35] and fluorene oligomers[36] have indeed shown that chain planarization leads to enhanced electronic delocalization and a concomitant reduction in configurational coordinate change per oscillator strength, resulting in a decrease in *S* with increasing oligomer length. We therefore conclude that, as the β-phase content in PFO films is increased, β-phase chain segments exhibit a more planar geometry and comprise a higher number of fluorene units associated with increased effective π-conjugation.

In addition to the emission spectra, we analyzed the changes in absorptance spectra of the PFO films that occur as the β-phase content is varied (Figure S1, S2). We observe that some of the trends are similar to those in emission, with the 0−0 absorption peak of the β-phase fraction clearly red-shifting with increasing β-phase fraction. However, we find that, whereas all β-phase emission spectra show a well-defined vibronic progression, the absorptance spectra seem to have broader emission beyond the 0−0 peak, and for the lower-phase fractions only the 0−0 peak is well-resolved (Figure S2). A possible reason for the apparent broadening of the β-phase absorption spectra lies in the method by which these were determined, which is commonly used across the field. The spectra are obtained by subtraction of the absorptance spectrum of a purely glassy reference film from the absorptance of a film containing both phases. A slight distortion in the obtained β-phase absorptance in a mixed film might arise if the reference spectrum does not exactly represent the glassy-phase absorptance in a mixed film. Small changes might, for example, be introduced by strain induced by the presence of the β-phase or selective conformation-dependent conversion of certain glassy to β-phase polymer chains (see further discussion in Supporting Information Section 2.3). We highlight that this would mainly be prominent at the onset of the glassy-phase absorption and not influence the 0−0 peak, which we used for the calculation of the Förster radius outlined below. As an alternative, these effects may result from small random fluctuations in the torsion angle between fluorene units within the β-phase, which have been shown to result in broadening in the absorption spectrum.[37,38] Both explanations highlight a strong dependence of the optical properties on film microstructure and therefore also emphasize the possibility that these may depend significantly on the preparation methods used.[39]

The possibility to enhance the PLQE of PFO thin films by tuning the β-phase fraction[13] provides a motive to further study the variation in PLQE for a set of samples, as prepared here, with systematically varying fraction. For each β-phase fraction, we experimentally determined the PLQE and PL lifetime, from which we derived the radiative and nonradiative decay rates of the exited state, as plotted in Figure 1c (details given in the Supporting Information). We find that, while the radiative decay rate increases as a function of increasing β-phase, the nonradiative rate decreases. The PLQE shows an increasing trend with increasing β-phase content in the film, with the PLQE value of 0.72 deduced here for the 25.6% β-phase sample being the highest PLQE value reported for a PFO film.

A change in PLQE with varying β-phase fraction has been observed previously,[8,13,26] with some authors[8,13] finding an increase with increasing β-phase content, followed by a decrease in PLQE at a β-phase content in excess of ∼10%, while others[26] reported no initial increase but still a decrease at higher β-phase fractions. While the reasons for such trends in PLQE as a function of β-phase content in PFO films were not fully explained, it has been assumed that both the β-phase fraction itself and the degree of dispersal of the β-phase chain segments within the glassy phase may play an important role.[13] Thus, film microstructure, which may also depend on the film preparation method, will influence the photophysical properties of PFO films. The range of PLQE values obtained by different authors[8,13,26] using different batches of polymer handled in different ways to prepare films and using different measurements therefore suggests that it is not only the β-phase percentage in the film that determines photophysical properties but that indeed the dispersion and arrangement of the β-phase chain segments may influence the observed trends with β-phase fraction. Importantly, we here use a single method for the preparation of a series of PFO films with varying β-phase content. We therefore believe that the changes we observe are closer to the intrinsic conformational changes resulting from this method. In particular, we propose that the increase in radiative and decrease in nonradiative decay rate may be closely linked to the planarization and enhancement in conjugation length we observe with increasing fraction of β-phase. With increasing conjugation length of the β-phase segments we expect an enhancement of oscillator strength, while planarization of the backbone may lead to a reduced

DOI: 10.1021/acs.jpclett.9b00483
J. Phys. Chem. Lett. 2019, 10, 1729−1736

intersystem crossing rate, possibly caused by the resulting decoupling of p and 2s orbitals, as reported for other π-conjugated molecules.[40] Therefore, the enhancement of the PLQE with increasing β-phase content may be directly linked with the accompanying conformational changes of the β-phase segments.

To unravel how the conformational changes with increasing β-phase content impact the energy transfer from glassy-phase chain segments to β-phase chain segments, we directly observed the dynamic of such transfers and analyzed it in terms of Förster theory. Originally developed by Theodor Förster to explain fluorescence depolarization in solutions,[41−43] this resonance energy transfer approach is based on dipole−dipole interactions between an energy donor (here, glassy-phase chain segments) and an energy acceptor (here, β-phase chain segments). The theory predicts an expected rate of energy transfer in terms of the Förster radius R_0, defined as the distance between donor and acceptor at which excitation energy transfer from the donor to the acceptor is as likely to happen as any other de-excitation of the donor.[42,43]

We first derive the apparent Förster radius from direct measurements of the PL decay transients, which reflect the actual transfer dynamics that may include additional processes, such as exciton diffusion within the host preceding the energy transfer. We then contrast these values of R_0 with those expected from the spectral overlap between donor emission and acceptor absorption according to Förster theory, which takes into account dipole−dipole coupling between donor and acceptor only. Both methods have been applied in isolation to PFO.[22,23,25] However, as the two approaches differ in their underlying assumptions, contrasting them for a single set of films enables us to examine directly the extent to which exciton diffusion and possible arrangement of the transition dipoles influence the energy transfer in the films. In addition, the use of a well-defined series of PFO films with a wide range of β-phase fractions, fabricated through a single processing method, allows us to gain new insights into how energy transfer in PFO films is affected by the conformational changes occurring with increasing β-phase content.

As the first step, we used time-resolved PL measurements to determine R_0 from the decay of the PL originating predominantly from the glassy phase. We measured the PL transients using the PL-upconversion technique, which enabled us to capture the ultrafast energy transfer dynamics in PFO with a 300 fs time resolution[22,44] (see Section S6 in the Supporting Information for full experimental details). From the resulting transients, shown in Figure 2a, we find that the amount of β-phase in the film determines the PL intensity decay rate. For the film containing only the glassy phase of PFO, the PL intensity was observed to be nearly constant over the first 17 ps of the excitation decay, which is in agreement with time-correlated single-photon counting (TCSPC) measurements showing a PL lifetime τ_g on the order of nanoseconds (see Supporting Information Section 5 for measurement of τ_g). In contrast, the presence of β-phase segments leads to a rapid energy transfer from the glassy-phase segments as evident from the fast decay of the PL collected near the peak emission of the glassy phase, consistent with observations reported in other studies for individual samples containing a specific β-phase fraction.[21,22] By extracting the value of R_0 from these data, we are able to investigate systematically how such varying β-phase fractions affect the energy transfer. We note that such an investigation is virtually impossible to perform from simple analysis of the PL emission spectra alone (Figure 1) given that transfer of excitations from the glassy to the β-phase clearly occurs with close to 100% efficiency even when only small percentages of β-phase are present.

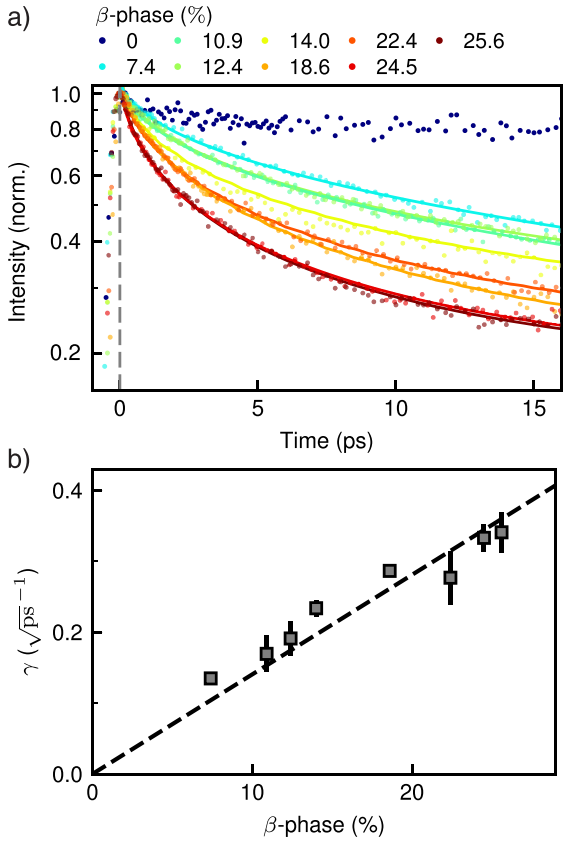

Figure 2. (a) Normalized transients of PL emitted at 419 nm from PFO films with varying β-phase content and detected by PL-upconversion following excitation at 405 nm, plotted with a fit obtained by using eq 4 based on Förster theory. (b) Fitting parameter γ reflecting the energy transfer dynamics from glassy to β-phase, plotted as a function of β-phase percentage. The dashed line is a guide and represents a linear variation through the origin.

The Förster radius R_0 can be derived from the PL transients by considering an ensemble average over all possible energy transfers from donors to acceptors, which are assumed to be spatially evenly distributed through the film.[42,45,46] Under the assumption of a dipole−dipole nature of the resonance energy transfer, R_0 is given by the following expression:

$$R_0 = \left(\frac{3}{2\pi^{3/2}} \frac{\sqrt{\tau_d}\gamma}{c_\beta} \right)^{1/3} \quad (1)$$

Here, τ_d denotes the excited-state lifetime of the donor (glassy phase) in absence of the acceptor (β-phase), which we determine from TCSPC measurements on a purely glassy sample (see Supporting Information Section 5), c_β is the density of β-phase chromophores, estimated from the chromophore density in a glassy-spin-coated film c_g[47] (see Supporting Information Section 6) and the fraction of β-phase within the film (β, see Supporting Information Section 2) as

$$c_\beta = \frac{\beta}{1-\beta} c_g \quad (2)$$

DOI: 10.1021/acs.jpclett.9b00483
J. Phys. Chem. Lett. 2019, 10, 1729−1736

The parameter γ captures the effective rate with which energy transfer occurs and is therefore obtained from analysis of the donor emission decay dynamics shown in Figure 2a. The films were excited at a wavelength of 405 nm, and the PL decay was recorded at 419 nm. At this wavelength, emission is dominated mostly by the donor glassy phase, leading to the observed rapid decay. However, to account for some spectrally overlapping contributions from the β-phase, we model the PL intensity as a sum of contributions from both glassy and β-phase chain segments:

$$I_{PL} = C_d n_d + C_a n_a \tag{3}$$

Here, in addition to the excited donor/acceptor populations $n_{d/a}$, the excitation and detection wavelengths influence the strength of the contributions to the PL intensity from each of the two phases, accounted for by C_d and C_a. From our emission data (Figure 1a), we expect a small contribution from the β-phase chain segments. In energy transfer studies, direct excitation of the acceptor molecules is often neglected according to an assumption that the acceptor concentration is small or that the acceptor does not absorb at the excitation wavelength. However, in our case we must account for direct acceptor excitation in our derivation, as there is a considerable amount of acceptors present in the film, and they absorb at 405 nm because of the vibronic progression (0−1, 0−2 peaks) above the 0−0 peak. Under these assumptions, the following expression is obtained for the total PL intensity (see Supporting Information Section 6.1.2 for a full derivation):

$$I_{PL}(t) = A\ \exp(-2\gamma\sqrt{t}) + B \tag{4}$$

with $A = (C_d - C_a)N_d$, and $B = C_a(N_d + N_a)$, where N_d and N_a denote the initial excited population of donors and acceptors, respectively. The PL intensity $I_{PL}(t)$ shows a square-root dependence on time, which accounts for the shape of the PL transients and is characteristic for resonant Förster energy transfer (see Supporting Information Figure S11) in a spatially random three-dimensional distribution of donor and acceptor dipoles. Fitting eq 4 to the transients hence allows for the extraction of γ, from which R_0 may be determined through eq 1 for every PFO film containing a given β-phase fraction.

Figure 2a shows the PL transients together with the corresponding fits, with the extracted variation of γ shown in part (b) as a function of β-phase fraction. As expected, γ tends to zero for low β-phase fraction; no energy transfer occurs in a purely glassy sample. We also observe an approximately linear relationship between γ and increasing β-phase content in the film. The increase in γ represents a more rapid PL decay consistent with faster energy transfer from glassy chain segments to β-phase chain segments for higher β-phase fractions. The Förster radius derived from these data takes into account both γ and the concentration of β-phase chain segments in the films, resulting in the slightly decreasing trend for R_0 with increasing β-phase content displayed in Figure 4 (blue open squares).

To assess how these Förster radii compare with those expected from Förster's theory of resonance energy transfer, we used the following expression to calculate R_0 from the overlap between the donor emission and the acceptor absorption:[32,48]

$$R_0 = \left(\frac{9\ \ln(10)\kappa^2\phi_d}{128\pi^5 N_A n^4} J\right)^{1/6} \tag{5}$$

where N_A is Avogadro's constant, ϕ_d is the PLQE of the glassy sample, n is the refractive index (set to $n = 1.6$[49,50]), $J = \int I_d(\lambda)\epsilon_a(\lambda)\lambda^4\,d\lambda$ is the overlap integral of the normalized donor fluorescence and the molar extinction coefficient of the acceptor, and κ denotes the geometric orientation factor of the donor and acceptor dipoles, defined as

$$\kappa = \vec{\mu_d}\cdot\vec{\mu_a} - 3(\vec{\mu_d}\cdot\overrightarrow{R_{da}})(\vec{\mu_a}\cdot\overrightarrow{R_{da}}) \tag{6}$$

Here, $\vec{R_{da}}$ is the normalized vector along the donor−acceptor separation direction, and $\vec{\mu_a}$ and $\vec{\mu_d}$ are the directions of the transition dipole moments of the acceptor and donor, respectively. In our calculation, we used $\kappa = 0.845 \times \sqrt{2/3}$, which corresponds to random but fixed relative orientations of donors and acceptors in a film.[45,51] The expression in eq 5 is derived for through-space resonant energy transfer based on Coulombic point dipole−dipole interactions between the energy donor and the acceptor[32,45,48] (see Supporting Information Section 6.2.1 for full details of these calculations). Energy conservation requires that the normalized donor fluorescence and the molar extinction coefficient spectra of the absorber overlap for the excitation energy transfer to be possible. We note that the red-shift of the β-phase peak of the molar extinction coefficient with increasing β-phase content causes a reduction of this overlap (Figure 3), because the 0−0 peak of the β-phase absorption shifts to wavelengths longer than that of the 0−0 peak of the glassy-phase absorption. This small reduction in the overlap integral hence leads to a slight decrease in the calculated Förster radius with increasing β-phase fraction (see red diamonds, Figure 4).

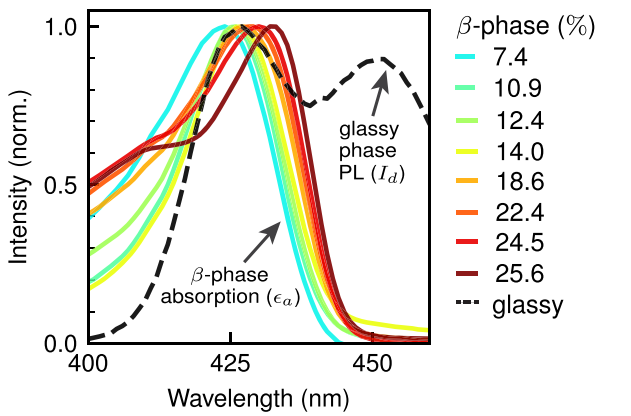

Figure 3. Overlap between the normalized emission (fluorescence, I_d) of the glassy phase and the absorption (molar extinction coefficient, ϵ_a) of the β-phase in thin films of PFO, shown for a range of different β-phase fractions.

We proceed to discuss the β-phase dependence of the resonant energy transfer and to compare the Förster radii obtained from spectral overlap and PL transients, displayed in Figure 4. For both calculation methods, we find that the value of R_0 decreases with increasing β-phase content as expected from our above computation of R_0 from spectral overlap. These correlations confirm that the changes in spectral overlap indeed cause R_0 to decline as the percentage of β-phase is increased, signifying that the resonance condition for the energy transfer between glassy and β-phase chain segments alters with varying β-phase content. However, despite the good agreement between general trends in R_0 as a function of β-phase content in the film, we find that the actual values of R_0

DOI: 10.1021/acs.jpclett.9b00483
J. Phys. Chem. Lett. 2019, 10, 1729−1736

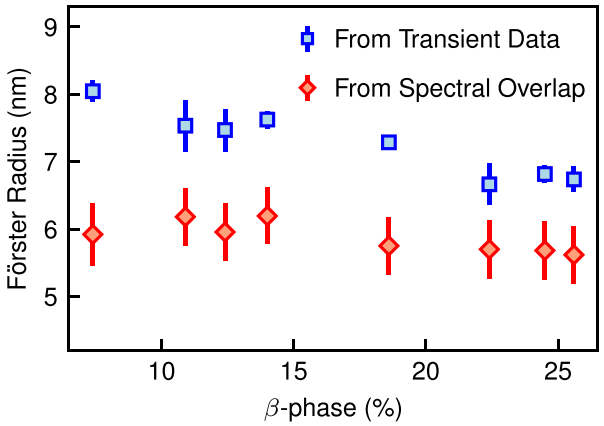

Figure 4. Förster radii for energy transfer between glassy and β-phase chains in PFO, plotted as a function of β-phase percentage. Values were derived from transient data (blue squares) and from the spectral overlap between glassy-phase (donor) emission and β-phase (acceptor) absorption (red diamonds).

derived from the PL transients are substantially higher than expected from the spectral overlap. We discuss below two possibilities for this discrepancy, which are the diffusion of excitons within the glassy matrix prior to energy transfer and a local alignment or correlation between transition dipole moments.

For the former mechanism, a dynamic migration of excitons within the glassy matrix may bring them effectively into closer proximity to β-phase segments than would be estimated from the β-phase segment concentration alone. We assume in our calculation of R_0 that the energy transfer occurs from an acceptor that was directly excited by the laser. An additional multiple-step exciton diffusion on or between glassy-phase chain segments (donors) prior to the energy transfer will increase the effectively experienced Förster radius[32] by allowing excitations to diffuse to within the capture radius of an acceptor. Exciton diffusion is captured in the PL dynamics only and can therefore account for the higher values of R_0 obtained from the PL transients. Exciton diffusion either occurs between segments on the same polymer chain (intrachain) or between chains (interchain), which both increase the Förster radius. Exciton diffusion in PFO films has also been observed elsewhere[23−26] and is therefore highly likely to contribute to the enhancement of Förster radii effectively experienced. We note that on-chain as well as interchain exciton diffusion processes are expected to be sensitive to small variations in chain conformation and film microstructure,[29,39,52] which again are susceptible to details of film preparation methods.[53,54]

As a second possible contribution, the difference in R_0 could be caused by some degree of local alignment between the donor and acceptor dipoles. We recall that we had assumed the transition dipoles to be oriented randomly when calculating R_0 from spectral overlap, using a value of $\kappa = 0.845 \times \sqrt{2/3}$ for the geometric orientation factor. This value was derived by Maksimov and Rozman[51] for fixed donors and acceptors in random positions and with randomly orientated transition dipole moments within a solid. However, the second assumption will not hold if some alignment or correlation between the orientation of adjacent chains exists. In the limiting case that all transition dipoles of donors and acceptors are oriented parallel to each other (still assuming random positions), the geometric orientation factor would take a value of $\kappa = 0.943 \times \sqrt{2/3}$,[51] which would increase R_0 by 0.2 to 0.25 nm. However, such a slight increase is too small to account for the much larger differences we observe between the values of R_0 derived from transients, and those expected from spectral overlap calculations (see Figure 4). We also note that such alignment of donor and acceptor dipoles would require a degree of local ordering, which is unlikely to be substantial inside these thin polymer films. For example, there is no evidence that isolated domains of locally aligned chains form, with the glassy and β-phase in PFO having been reported to be well-intermixed,[23,28] in agreement with the complete energy transfer we observe here. It is theoretically possible that a glassy-phase chain segment formed adjacent to a β-phase segment as part of the same chain exhibit a local correlation between transition dipole orientation. However, intrachain energy transfer will be less efficient than interchain transfer, because of the closer proximities in the latter case. Either way, such local correlations between dipole orientations will only give rise to minute increases in the expected Förster radii, making it unlikely that they can account for the observed boost in R_0. We therefore conclude that the enhancement of the observed energy transfer must originate from the assistance of exciton diffusion within the glassy phase prior to energy transfer.

Finally, we note that, while both the PLQE (Figure 1c) and the energy transfer parameter γ (Figure 2b) similarly increase with β-phase content of the PFO film, these two trends are not directly linked. As the PL spectra of the films (Figure 1a) show, the energy transfer efficiency is close to 100% even for films containing a low percentage of β-phase; no glassy-phase emission can be detected. Therefore, while the speed of transfer increases with increasing β-phase fraction, almost all excitations still transfer from the glassy to the β-phase before they are able to recombine. The rise in PLQE with β-phase fraction is therefore governed exclusively by the planarization and extension of β-phase chromophores as the fraction of β-phase in the film is increased, as discussed above.

In conclusion, we have investigated how the fraction of β-phase chains present in PFO thin films affects the nature of the electronic states, chain conformation, and the Förster resonant energy transfer from glassy to β-phase chain segments. We ensured consistency among PFO films by employing the same fabrication technique to obtain a wide range of β-phase fractions. We demonstrated that such comparability is of great importance, as photophysical properties of PFO films are very sensitive to film microstructure and therefore to film preparation. All PFO films fabricated exhibited high (>0.6 for the films containing β-phase) PLQE, peaking at a value of 0.72 at 25.6% β-phase content. We observed that, with increasing β-phase content, the emission peaks of the β-phase red-shift and narrow, while the associated Huang−Rhys factor decreases. These findings suggest that the conformation of β-phase segments changes with increasing fraction, adopting a more planar structure and/or including a larger number of repeat units. The red-shift also affects the resonance condition for energy transfer between glassy-phase and β-phase chain segments resulting in a slight decrease in Förster radius with increasing β-phase fraction. Comparing the Förster radii obtained from spectral overlap calculations to those extracted from measurements of transient PL dynamics, we find that the Förster radius is enhanced by exciton diffusion within the glassy phase occurring prior to energy transfer. The insights

DOI: 10.1021/acs.jpclett.9b00483
J. Phys. Chem. Lett. 2019, 10, 1729−1736

obtained from this systematic study deepen the understanding of the fundamental photophysical properties of PFO films, which is essential for the further development of light-emitting materials and applications.

■ ASSOCIATED CONTENT

Supporting Information

The Supporting Information is available free of charge on the ACS Publications website at DOI: 10.1021/acs.jpclett.9b00483.

Sample preparation, experimental procedures, and detailed results for absorption spectra and determination of β-phase content, time-integrated photoluminescence spectra, photoluminescence quantum efficiency, lifetimes and decay rates, Förster radii (PDF)

■ AUTHOR INFORMATION

Corresponding Author

E-mail: laura.herz@physics.ox.ac.uk.

ORCID

Hannah J. Eggimann: 0000-0001-5901-9425

Laura M. Herz: 0000-0001-9621-334X

Notes

The authors declare no competing financial interest.

■ ACKNOWLEDGMENTS

The authors thank Prof. D. D. C. Bradley for the helpful scientific discussions on this work. The authors acknowledge support by the University of Oxford and by the U.K. Engineering and Physical Sciences Research Council. H.J.E. thanks the Fondation Zdenek and Michaela Bakala for support through their scholarship. F.L.R. further thanks Wolfson College and Dr. S. Harrison for the award of a Wolfson Harrison U.K. Research Council Physics Scholarship.

■ REFERENCES

(1) Chiang, C. K.; Fincher, C. R.; Park, Y. W.; Heeger, A. J.; Shirakawa, H.; Louis, E. J.; Gau, S. C.; MacDiarmid, A. G. Electrical Conductivity in Doped Polyacetylene. *Phys. Rev. Lett.* **1977**, *39*, 1098−1101.

(2) Tang, C. W.; van Slyke, S. A. Organic Electroluminescent Diodes. *Appl. Phys. Lett.* **1987**, *51*, 913−915.

(3) Burroughes, J. H.; Bradley, D. D. C.; Brown, A. R.; Marks, R. N.; Mackay, K.; Friend, R. H.; Burns, P. L.; Holmes, A. B. Light-Emitting Diodes Based on Conjugated Polymers. *Nature* **1990**, *347*, 539−541.

(4) Kraft, A.; Grimsdale, A. C.; Holmes, A. B. Electroluminescent Conjugated Polymers-Seeing Polymers in a New Light. *Angew. Chem., Int. Ed.* **1998**, *37*, 402−428.

(5) Guo, X.; Baumgarten, M.; Müllen, K. Designing Pi-Conjugated Polymers for Organic Electronics. *Prog. Polym. Sci.* **2013**, *38*, 1832−1908.

(6) Grice, A. W.; Bradley, D. D. C.; Bernius, M. T.; Inbasekaran, M.; Wu, W. W.; Woo, E. P. High Brightness and Efficiency Blue Light-Emitting Polymer Diodes. *Appl. Phys. Lett.* **1998**, *73*, 629−631.

(7) Zhang, X.; Hu, Q.; Lin, J.; Lei, Z.; Guo, X.; Xie, L.; Lai, W.; Huang, W. Efficient and Stable Deep Blue Polymer Light-Emitting Devices Based on β-Phase Poly(9,9-dioctylfluorene). *Appl. Phys. Lett.* **2013**, *103*, 153301.

(8) Zhang, Q.; Chi, L.; Hai, G.; Fang, Y.; Li, X.; Xia, R.; Huang, W.; Gu, E. An Easy Approach to Control β-Phase Formation in PFO Films for Optimized Emission Properties. *Molecules* **2017**, *22*, 315.

(9) Chua, L. L.; Zaumseil, J.; Chang, J. F.; Ou, E. C. W.; Ho, P. K. H.; Sirringhaus, H.; Friend, R. H. General Observation of n-Type Field-Effect Behaviour in Organic Semiconductors. *Nature* **2005**, *434*, 194−199.

(10) Heliotis, G.; Xia, R.; Bradley, D. D. C.; Turnbull, G. A.; Samuel, I. D.; Andrew, P.; Barnes, W. L. Blue, Surface-Emitting, Distributed Feedback Polyfluorene Lasers. *Appl. Phys. Lett.* **2003**, *83*, 2118−2120.

(11) Rothe, C.; Galbrecht, F.; Scherf, U.; Monkman, A. The β-Phase of Poly(9,9-dioctylfluorene) as a Potential System for Electrically Pumped Organic Lasing. *Adv. Mater.* **2006**, *18*, 2137−2140.

(12) Lu, H.-H.; Liu, C.-Y.; Chang, C.-H.; Chen, S.-A. Self-Dopant Formation in Poly(9,9-di-n-octylfluorene) via a Dipping Method for Efficient and Stable Pure-Blue Electroluminescence. *Adv. Mater.* **2007**, *19*, 2574−2579.

(13) Perevedentsev, A.; Chander, N.; Kim, J.-S. S.; Bradley, D. D. C. Spectroscopic Properties of Poly(9,9-dioctylfluorene) Thin Films Possessing Varied Fractions of β-Phase Chain Segments: Enhanced Photoluminescence Efficiency via Conformation Structuring. *J. Polym. Sci., Part B: Polym. Phys.* **2016**, *54*, 1995−2006.

(14) Yap, B. K.; Xia, R.; Campoy-Quiles, M.; Stavrinou, P. N.; Bradley, D. D. C. Simultaneous Optimization of Charge-Carrier Mobility and Optical Gain in Semiconducting Polymer Films. *Nat. Mater.* **2008**, *7*, 376−380.

(15) Bradley, D. D. C.; Grell, M.; Long, X.; Mellor, H.; Grice, A.; Inbasekaran, M.; Woo, E. P. Influence of Aggregation on the Optical Properties of a Polyfluorene. *Proc. SPIE* **1997**, *3145*, 254−259.

(16) Grell, M.; Bradley, D. D. C.; Ungar, G.; Hill, J.; Whitehead, K. S. Interplay of Physical Structure and Photophysics for a Liquid Crystalline Polyfluorene. *Macromolecules* **1999**, *32*, 5810−5817.

(17) Scherf, U.; List, E. J. W. Semiconducting Polyfluorenes - Towards Reliable Structure-Property Relationships. *Adv. Mater.* **2002**, *14*, 477−487.

(18) Ariu, M.; Lidzey, D. G.; Sims, M.; Cadby, A. J.; Lane, P. A.; Bradley, D. D. C. The Effect of Morphology on the Temperature-Dependent Photoluminescence Quantum Efficiency of the Conjugated Polymer Poly(9, 9-dioctylfluorene). *J. Phys.: Condens. Matter* **2002**, *14*, 9975−9986.

(19) Monkman, A.; Rothe, C.; King, S.; Dias, F. Polyfluorene Photophysics. *Adv. Polym. Sci.* **2008**, *212*, 187−225.

(20) Sirtonski, M. R.; McFarlane, S. L.; Veinot, J. G. Stabilizing the Optical Properties of PFO Through Addition of a Non-Volatile Low Molecular Weight Aromatic Ether. *J. Mater. Chem.* **2010**, *20*, 8147−8152.

(21) Ariu, M.; Sims, M.; Rahn, M.; Hill, J.; Fox, A. M.; Lidzey, D. G.; Oda, M.; Cabanillas-Gonzalez, J.; Bradley, D. D. C. Exciton Migration in β-Phase Poly(9,9-dioctylfluorene). *Phys. Rev. B: Condens. Matter Mater. Phys.* **2003**, *67*, 1−11.

(22) Khan, A. L. T.; Sreearunothai, P.; Herz, L. M.; Banach, M. J.; Köhler, A. Morphology-Dependent Energy Transfer Within Polyfluorene Thin Films. *Phys. Rev. B: Condens. Matter Mater. Phys.* **2004**, *69*, No. 085201.

(23) Shaw, P. E.; Ruseckas, A.; Peet, J.; Bazan, G. C.; Samuel, I. D. W. Exciton-Exciton Annihilation in Mixed-Phase Polyfluorene Films. *Adv. Funct. Mater.* **2010**, *20*, 155−161.

(24) Denis, J.-C.; Schumacher, S.; Hedley, G. J.; Ruseckas, A.; Morawska, P. O.; Wang, Y.; Allard, S.; Scherf, U.; Turnbull, G. A.; Samuel, I. D. W.; et al. Subpicosecond Exciton Dynamics in Polyfluorene Films from Experiment and Microscopic Theory. *J. Phys. Chem. C* **2015**, *119*, 9734−9744.

(25) Montilla, F.; Ruseckas, A.; Samuel, I. D. W. Exciton-Polaron Interactions in Polyfluorene Films with β-Phase. *J. Phys. Chem. C* **2018**, *122*, 9766−9772.

(26) Bansal, A. K.; Ruseckas, A.; Shaw, P. E.; Samuel, I. D. W. Fluorescence Quenchers in Mixed Phase Polyfluorene Films. *J. Phys. Chem. C* **2010**, *114*, 17864−17867.

(27) Peet, J.; Brocker, E.; Xu, Y.; Bazan, G. C. Controlled Beta-Phase Formation in Poly(9,9-di-n-octylfluorene) by Processing with Alkyl Additives. *Adv. Mater.* **2008**, *20*, 1882−1885.

(28) Yu, M. N.; Soleimaninejad, H.; Lin, J. Y.; Zuo, Z. Y.; Liu, B.; Bo, Y. F.; Bai, L. B.; Han, Y. M.; Smith, T. A.; Xu, M.; et al.

DOI: 10.1021/acs.jpclett.9b00483
J. Phys. Chem. Lett. 2019, 10, 1729−1736

Photophysical and Fluorescence Anisotropic Behavior of Polyfluorene β-Conformation Films. *J. Phys. Chem. Lett.* **2018**, *9*, 364−372.
(29) Schwartz, B. J. Conjugated Polymers as Molecular Materials: How Chain Conformation and Film Morphology Influence Energy Transfer and Interchain Interactions. *Annu. Rev. Phys. Chem.* **2003**, *54*, 141−172.
(30) Huang, L.; Huang, X.; Sun, G.; Gu, C.; Lu, D.; Ma, Y. Study of β-Phase and Chains Aggregation Degrees in Poly(9,9-dioctylfluorene) (PFO) Solution. *J. Phys. Chem. C* **2012**, *116*, 7993−7999.
(31) Chang, M. H.; Hoffmann, M.; Anderson, H. L.; Herz, L. M. Dynamics of Excited-State Conformational Relaxation and Electronic Delocalization in Conjugated Porphyrin Oligomers. *J. Am. Chem. Soc.* **2008**, *130*, 10171−10178.
(32) Köhler, A.; Bässler, H. *Electronic Processes in Organic Semiconductors;* WileyVCH Verlag GmbH: Weinheim, Germany, 2015.
(33) Brown, P. J.; Thomas, D. S.; Köhler, A.; Wilson, J. S.; Kim, J. S.; Ramsdale, C. M.; Sirringhaus, H.; Friend, R. H. Effect of Interchain Interactions on the Absorption and Emission of Poly(3-hexylthiophene). *Phys. Rev. B: Condens. Matter Mater. Phys.* **2003**, *67*, No. 064203.
(34) Hoffmann, S. T.; Scheler, E.; Koenen, J. M.; Forster, M.; Scherf, U.; Strohriegl, P.; Bässler, H.; Köhler, A. Triplet Energy Transfer in Conjugated Polymers. III. An Experimental Assessment Regarding the Influence of Disorder on Polaronic Transport. *Phys. Rev. B: Condens. Matter Mater. Phys.* **2010**, *81*, 165208.
(35) Cornil, J.; Beljonne, D.; Heller, C. M.; Campbell, I. H.; Laurich, B. K.; Smith, D. L.; Bradley, D. D. C.; Müllen, K.; Brédas, J. L. Photoluminescence Spectra of Oligo-Paraphenylenevinylenes: A Joint Theoretical and Experimental Characterization. *Chem. Phys. Lett.* **1997**, *278*, 139−145.
(36) Wasserberg, D.; Dudek, S. P.; Meskers, S. C.; Janssen, R. A. Comparison of the Chain Length Dependence of the Singlet- and Triplet-Excited States of Oligofluorenes. *Chem. Phys. Lett.* **2005**, *411*, 273−277.
(37) Huber, D. L.; Avgin, I. Optical Absorption of the β-Phase of Poly(9,9-dioctylfluorene). *J. Polym. Sci., Part B: Polym. Phys.* **2016**, *54*, 1109−1111.
(38) Avgin, I.; Huber, D. L. Excitons in Disordered Polymers. *J. Lumin.* **2007**, *122−123*, 389−392.
(39) Silva, C.; Russell, D. M.; Dhoot, A. S.; Herz, L. M.; Daniel, C.; Greenham, N. C.; Arias, A. C.; Setayesh, S.; Müllen, K.; Friend, R. H. Exciton and Polaron Dynamics in a Step-Ladder Polymeric Semiconductor: The Influence of Interchain Order. *J. Phys.: Condens. Matter* **2002**, *14*, 9803−9824.
(40) Nijegorodov, N. I.; Downey, W. S. The Influence of Planarity and Rigidity on the Absorption and Fluorescence Parameters and Intersystem Crossing Rate Constant in Aromatic Molecules. *J. Phys. Chem.* **1994**, *98*, 5639−5643.
(41) Förster, T. Energiewanderung und Fluoreszenz. *Naturwissenschaften* **1946**, *33* (6), 166−175.
(42) Förster, T. Experimentelle und Theoretische Untersuchung des Zwischenmolekularen Übergangs von Elektroneneanregungsenergie. *Z. Naturforsch.* **1949**, *4a*, 321−327.
(43) Förster, T. 10th Spiers Memorial Lecture. Transfer Mechanisms of Electronic Excitation. *Discuss. Faraday Soc.* **1959**, *27*, 7−17.
(44) Chang, M. H.; Frampton, M. J.; Anderson, H. L.; Herz, L. M. Intermolecular Interaction Effects on the Ultrafast Depolarization of the Optical Emission from Conjugated Polymers. *Phys. Rev. Lett.* **2007**, *98*, No. 027402.
(45) Herz, L. M.; Silva, C.; Friend, R. H.; Phillips, R. T.; Setayesh, S.; Becker, S.; Marsitsky, D.; Müllen, K. Effects of Aggregation on the Excitation Transfer in Perylene-End-Capped Polyindenofluorene Studied by Time-Resolved Photoluminescence Spectroscopy. *Phys. Rev. B: Condens. Matter Mater. Phys.* **2001**, *64*, 195203.
(46) Powell, R. C.; Soos, Z. G. Singlet Exciton Energy Transfer in Organic Solids. *J. Lumin.* **1975**, *11*, 1−45.
(47) Stevens, M. A.; Silva, C.; Russell, D. M.; Friend, R. H. Exciton Dissociation Mechanisms in the Polymeric Semiconductors Poly(9,9-dioctylfluorene) and Poly(9,9-dioctylfluorene-co-benzothiadiazole). *Phys. Rev. B: Condens. Matter Mater. Phys.* **2001**, *63*, 165213.
(48) Medintz, I., Hildebrandt, N., Eds. *FRET-Förster Resonance Energy Transfer;* Wiley-VCH Verlag GmbH & Co.KGaA: Weinheim, Germany, 2014.
(49) Macdonald, E. K.; Shaver, M. P. Intrinsic High Refractive Index Polymers. *Polym. Int.* **2015**, *64*, 6−14.
(50) Campoy-Quiles, M.; Heliotis, G.; Xia, R.; Ariu, M.; Pintani, M.; Etchegoin, P.; Bradley, D. D. Ellipsometric Characterization of the Optical Constants of Polyfluorene Gain Media. *Adv. Funct. Mater.* **2005**, *15*, 925−933.
(51) Maksimov, M.; Rozman, I. On Energy Transfer in Solid Solutions. *Opt. Spectrosc. USSR* **1961**, *12*, 337−338.
(52) Collini, E.; Scholes, G. D. Coherent Intrachain Energy Migration in a Conjugated Polymer at Room Temperature. *Science* **2009**, *323*, 369−373.
(53) Perevedentsev, A.; Stavrinou, P. N.; Smith, P.; Bradley, D. D. C. Solution-Crystallization and Related Phenomena in 9,9-Dialkyl-Fluorene Polymers. II. Influence of Side-Chain Structure. *J. Polym. Sci., Part B: Polym. Phys.* **2015**, *53*, 1492−1506.
(54) Reichenberger, M.; Kroh, D.; Matrone, G. M. M.; Schötz, K.; Pröller, S.; Filonik, O.; Thordardottir, M. E.; Herzig, E. M.; Bässler, H.; Stingelin, N.; et al. Controlling Aggregate Formation in Conjugated Polymers by Spin-Coating Below the Critical Temperature of the Disorder-Order Transition. *J. Polym. Sci., Part B: Polym. Phys.* **2018**, *56*, 532−542.

DOI: 10.1021/acs.jpclett.9b00483
J. Phys. Chem. Lett. 2019, 10, 1729−1736